Amorphous solid dispersions of amphiphilic polymer excipients and indomethacin prepared by hot melt extrusion

*Larissa Keßler[1], Rashmi Mishra[2], Sami Hietala[3], Manon Lammens[2,8], Thomas Rades[4], Bert van Veen[5], Anne Juppo[2], Timo Laaksonen[6,7], Clare Strachan[2], Robert Luxenhofer[1]**

[1]Soft Matter Chemistry, Department of Chemistry, and Helsinki Institute of Sustainability Science, Faculty of Science, University of Helsinki, 00014 Helsinki, Finland
[2]Division of Pharmaceutical Chemistry and Technology, Faculty of Pharmacy, University of Helsinki, 00790 Helsinki, Finland
[3]Department of Chemistry, University of Helsinki, P.O. Box 55, FIN-00014 Helsinki, Finland
[4]Department of Pharmacy, University of Copenhagen, 2100 Copenhagen, Denmark
[5]Pharmaceutical Sciences, Orion Corporation, 02200 Espoo, Finland
[6]Division of Pharmaceutical Biosciences, Faculty of Pharmacy, University of Helsinki, 00790 Helsinki, Finland
[7]Faculty of Engineering and Natural Sciences, Tampere University, 33101 Tampere, Finland
[8]Laboratory of Pharmaceutical Technology, Ghent University, 9000 Ghent, Belgium

correspondence to: Prof. Dr. R. Luxenhofer: robert.luxenhofer@helsinki.fi

Keywords

amphiphilic block copolymer, poly(2-oxazoline), poly(2-oxazine), drug formulation, poly(vinyl pyrrolidone), poly(vinyl pyrrolidone-co-vinyl acetate)

Abstract

Improving the solubility of poorly water-soluble drugs is essential for enhancing bioavailability, formulation flexibility and reducing patient-to-patient variability. The preparation of amorphous solid dispersions (ASDs) is an attractive strategy to formulate such drugs, leading to higher apparent water solubility and therefore higher bioavailability. For such ASDs, water-soluble polymer excipients, such as poly(vinyl pyrrolidone) (PVP) or poly(vinyl pyrrolidone-co-vinyl acetate) (P(VP-co-VA)), are employed to solubilize and stabilize the drug against crystallization. We posit that polymers bearing tertiary amides are particularly well suited to stabilizing drugs containing H-bond donors, as they offer strong H-bonding potential between the polymer and drug. The aim of this study was to compare new and established polymers with tertiary amides as excipients for ASDs. Experimental amphiphilic ABA triblock copolymers comprising poly(2-methyl-2-oxazoline) (pMeOx), poly(2-butyl-2-oxazoline) (pBuOx) and poly(2-butyl-2-oxazine) (pBuOzi) blocks, were compared with the established excipients, PVP and P(VP-co-VA). ASDs with indomethacin as the model drug were prepared at high drug loadings via hot melt extrusion. The extrudates were studied with DSC and PXRD, revealing the ASDs to be fully amorphous up to 75wt% indomethacin, independent of the polymer used. ^{13}C CPMAS NMR provided insights into intermolecular associations as a function of drug loading, and suggested the presence of drug dimers at 75wt% drug loading in pMeOx-pBuOzi-pMeOx and pMeOx-pBuOx-pMeOx, which could affect physical stability. Independent of the polymers, the solid-state form of the drug in the ASD was found to affect the dissolution profile of the samples, insofar as the samples containing crystalline indomethacin showed slower dissolution than the fully amorphous ones. This study shows that the polymers comprising poly(2-oxazoline) and poly(2-oxazine) are effective polymers for ASD preparation, similar to PVP and P(VP-co-VA) which merits futher investigations into these novel polymers for formulating ASDs.

1 Introduction

A large proportion of new drugs and drug candidates exhibit very low water solubility.[1] This poses a significant challenge to the pharmaceutical industry and a variety of different formulation strategies are employed to overcome this solubility challenge.[2-3] The amorphous form with its disordered structure has a higher free energy (in lieu of the lattice stabilization) compared to the crystalline form, resulting in a higher apparent solubility, dissolution rate and potentially oral absorption of the drug.[4] Due to the thermodynamically favorable transition towards the lower energy crystalline state rendering the amorphous form physically unstable, pure amorphous drug forms are rarely used on their own. Addition of an excipient (usually a polymer) to form an amorphous solid dispersion can stabilize the drug against crystallization during both processing and storage.[5] Often, the added polymer inhibits recrystallization through, *inter alia*, reducing the molecular mobility of the drug and/or forming hydrogen bonds with the drug in a single phase system with molecular mixing of the components.[6-7] Furthermore, the excipient can modulate the dissolution profile of the drug and inhibit crystallization after dissolution.[8] Depending on the properties of the drug and polymer, different methods can be used for the preparation of ASDs, with hot melt extrusion (HME) and spray drying being the most important and widely used processes in industry.[9-10]

HME is a continuous and single-step process, which does not require the use of any solvent and is therefore considered more sustainable compared to spray drying. It involves the mixing and melting of the excipient and drug with subsequent extrusion.[9] Well-known and studied polymers for HME and used in multiple commercial products are, *inter alia*, hydroxypropyl methylcellulose (HPMC)[11-12], HPMC derivates[13], poly(vinyl pyrrolidone) (PVP)[14] and poly(vinyl pyrrolidone-co-vinyl acetate) (P(VP-co-VA))[15]. Apart from these well-established polymers, Soluplus®[16-17] has been introduced specifically for HME and other experimental excipients, such as poly(2-ethyl-2-oxazoline)[18] and ABA triblock copolymers comprising poly(2-oxazoline) (POx) and poly(2-oxazine) (POzi)[19] moieties, have been studied for HME more recently. Interestingly, PVP and P(VP-co-VA), are structurally similar to Soluplus® and POx/POzi based polymers, in that they all contain tertiary amide groups in their repeating units, which may act as hydrogen bond acceptors (but not H-donors) for the drug. However, unlike PVP and P(VP-co-VA), the POx/POzi based amphiphilic ABA triblock copolymers form well-defined micelles in aqueous solution.[20-21] Previously, the latter have been explored in high drug loading polymeric nanoformulations with drug loadings of more than 50wt% [20, 22-29], as well as stabilization of drug nano- and microparticles[30]. In the spring-and-parachute model often described for ASDs, the ASD serves as the spring, while the *in situ* formed micelles serve as a parachute by increasing the apparent aqueous solubility of the drug. The drug loaded micelles can remain colloidally stable over a period of up to several

months, as previously shown for a variety of drugs with the POx/POzi platform.[20] In particular, polymers containing poly(2-methyl-2-oxazoline) (pMeOx) as the A block and poly(2-butyl-2-oxazoline) (pBuOx) and poly(2-butyl-2-oxazine) (pBuOzi), as the B block, have been used successfully in high drug loading micellar formulations[20, 23, 31], stabilization of drug nanocrystals[30] and drug loaded microneedles[32]. It should be noted that, for some POx/POzi systems, a reasonably good drug loading capacity (albeit lower than for triblocks) can be achieved by changing the polymer structure to diblock, random or gradient copolymers.[33-35]

In this study, the amphiphilic ABA triblock copolymers pMeOx-pBuOzi-pMeOx and pMeOx-pBuOx-pMeOx were investigated as excipients for the preparation of ASDs with indomethacin (IND) as a model drug in different drug loadings, ranging from 25wt% to 80wt% and HME as an industrially relevant processing method. IND is often used as a model drug for the development of ASDs.[19, 36-38] The goal of this study is to compare the performance of the POx and POzi based polymers to the industrially used PVP and P(VP-co-VA) as crystallization inhibiting excipients in ASDs at very high drug loadings. To do so, the prepared extrudates were analyzed by DSC, PXRD and solid-state NMR measurements. Furthermore, the dissolution behavior as a function of both polymers and drug loading was evaluated.

2 Materials and Methods

2.1 Materials

Indomethacin (IND) was purchased from TCI chemicals (Zwijndrecht, Belgium), 3-amino-propanol, 2-aminoethanol, valeronitrile, 2-methyl-2-oxazoline, benzonitrile, calcium hydride, phosphorus pentoxide, methyl triflate and zinc acetate dihydrate were obtained from Sigma-Aldrich (Helsinki, Finland). Poly(vinyl pyrrolidone) (PVP) and poly(vinyl pyrrolidone-co-vinyl acetate) (P(VP-co-VA)) were purchased from BASF (Ludwigshafen, Germany). All materials were used as received unless otherwise stated.

The monomer 2-methyl-2-oxazoline was dried by stirring over CaH_2 under inert atmosphere, followed by distillation prior to use. Benzonitrile was dried by refluxing over P_2O_5 under inert atmosphere, followed by distillation prior to use.

2.2 Monomer Synthesis

The monomers 2-*n*-butyl-2-oxazoline (BuOx) and 2-*n*-butyl-2-oxazine (BuOzi) were synthesized following the procedure by Witte and Seeliger.[39] Briefly, in a nitrogen flushed flask, valeronitrile, 3-amino-propanol (for the 2-oxazine synthesis or 2-amino-ethanol for the 2-oxazoline synthesis) and catalytic amounts of zinc acetate dihydrate were mixed and heated to 130 °C for several days and the progress was controlled by ^{1}H NMR spectroscopy. After completion of the reaction, the mixture was dissolved in dichloromethane and washed three times with H_2O. The organic layer was dried with Na_2SO_4 and concentrated. The raw product was dried with CaH_2 and distilled under reduced pressure and nitrogen atmosphere to yield the product as a colourless liquid. Details can be found in the Supporting Information (Figure S1 – S2, Table S1 – S2).

2.3 Polymer Synthesis

The polymer synthesis and workup procedures were carried out as described elsewhere.[23] A more detailed description can be found in the Supporting Information (Figure S3 – S4, Table S3 – S4). Briefly, the methyl triflate was added to a dried and nitrogen-flushed Schlenk flask and dissolved in the respective amount of benzonitrile. The monomer 2-methyl-2-oxazoline was added, and the reaction mixture was heated to 120 °C and stirred until complete consumption of the monomer. The reaction was monitored by ^{1}H NMR spectroscopy. After full consumption of MeOx, the mixture was cooled to room temperature and the monomer for the second block, 2-*n*-butyl-2-oxazine or 2-*n*-butyl-2-oxazoline, was added. The mixture was heated to 130 °C overnight. The same procedure was repeated for the third block (MeOx). After confirmation of monomer consumption by ^{1}H NMR, the polymerization was terminated by addition of ethyl isonipecotate at 50 °C for 4 h. The solvent was removed under reduced

pressure. The polymer was transferred into a dialysis bag (MWCO 1 kDa, cellulose acetate, Spektrum™, Rancho Dominguez, CA, USA) and dialysed against deionized water for two days with several water changes. Afterwards, the solution was recovered from the bag and lyophilized.

2.4 Nuclear Magnetic Resonance Spectroscopy (NMR)

^{1}H NMR spectra were measured with an Avance III 500 MHz spectrometer from Bruker Biospin (Ettlingen, Germany) at a temperature of 25 °C (298 K). The spectra were calibrated on the solvent signal of CD_2Cl_2 (5.32 ppm). Solid state ^{13}C CPMAS NMR spectra were obtained with an Avance III 500 MHz spectrometer from Bruker Biospin (Ettlingen, Germany) using a double resonance CPMAS probe head. Samples were packed into 4 mm o.d. ZrO_2 rotors, plugged with KEL-F endcaps and spun at spinning frequency of 12 kHz. The length of the contact time for cross-polarization was 2 ms and the cross-polarization amplitude was linearly ramped from 70% to maximum amplitude. During the acquisition the protons were decoupled using SPINAL-64 decoupling. At least 2048 scans were collected with a 5 s relaxation delay and the spectra were externally referenced to adamantane.

2.5 Size Exclusion Chromatography (SEC)

SEC was performed using a Waters Acquity APC system, equipped with Acquity Column Manager – S, Sample Manager – pFTN, Isocratic Solvent Manager, Acquity RI Detector and Aquity TUV Detector (Waters Corporation, Milford, MA, USA). Acquity APC XT 45, 125 and 200 columns were used. The eluent was dimethylformamide (DMF, Fisher Scientific, Vantaa, Finland) with a flow of 0.6 mL/min and at a temperature of 40 °C. The system was calibrated with poly(methyl methacrylate) (PMMA) standards (Polymer Standard Service, Agilent, Espoo, Finland). The data was analysed using Empower 3 and OriginPro (OriginLab Corporation, Northampton, MA, USA).

2.6 Differential Scanning Calorimetry (DSC)

DSC was conducted using a DSC Q2000 (TA Instruments, Newcastle, DE, USA). Samples of about 5 mg were prepared in sealed aluminium pans and heated from +5 °C to +200 °C and subsequently cooled to −50 °C at a linear rate of 10 °C min^{-1} in a nitrogen atmosphere. This cycle was repeated three times, with a final cooling to room temperature. The glass transition temperature (T_g) was obtained from the inflection point of the second heating cycle and the melt temperature (T_m) is the peak maximum of the endothermic curve in the first heating. For modulated DSC measurements the samples were equilibrated at +5 °C for 5 min followed by a temperature ramp from +5 °C to +200 °C with a modulated heating rate of 3 °C min^{-1} with a frequency of ±1 °C every 60 s. The data was evaluated using Origin software.

2.7 Powder X-Ray Diffraction (PXRD)

Diffraction patterns of IND and polymer and polymer/IND extrudates were obtained using an EMPYREAN X-Ray diffractometer (Malvern PANalytical, Espoo, Finland) equipped with a transmission measurement geometry at room temperature and a voltage of 45 kV. The samples were scanned between 5 ° and 40° 2θ with a step size of 0.013° 2θ and a step time of 49.47 s. The ground samples were placed between two slices of Kapton tape and mounted on a transmission sample holder. The diffractograms were evaluated using Origin software.

Variable temperature PXRD measurements were conducted on a PANalytical X'Pert Pro MPD diffractometer (Malvern PANalytical, Espoo, Finland) equipped with an Anton Paar HTK1200N oven (Wundschuh, Austria) using Cu *K*α radiation. *In vacuo* measurements were conducted at $<10^{-3}$ mbar. The temperature was raised in 5 °C steps from 25 to 200 °C, with the measurements performed after equilibration of each step. The diffractograms were evaluated using Origin software.

2.8 Hot melt extrusion HME

HME was carried out on a ZE 9 HMI extruder (Three-Tec GmbH, Seon, Switzerland). The screw speed was set to 20 or 30 rpm for the whole extrusion process. Detailed information can be found in the Supporting Information (Table S5 – S8). The total amount of sample was around 5 g, which did not allow the use of continuous feeding during the extrusion process. Therefore, manual feeding of the extruder was conducted.

2.9 Ultraviolet-Visible (UV-Vis) Spectroscopy

UV-Vis experiments were performed on a JASCO V-750 UV-Vis spectrometer (JASCO UK Ltd., Heckmondwike, UK) equipped with a JASCO CTU-100 water jacketed Peltier thermostat system at a wavelength of 320 nm and a temperature of 25°C. A standard curve for IND was obtained by quantifying known amounts (Supporting Information, Figure S5). Data was analysed using Origin software.

2.10 Dissolution study – sink conditions

Dissolution tests were performed with a United States Pharmacopeia (USP) dissolution apparatus 2 with the rotational speed set at 50 rpm and the temperature at 37°C. The dissolution medium was 600 mL phosphate buffer solution (pH = 6.8) (Ph. Eur.). Three 1 cm extrudate pieces were weighed and added to the dissolution medium. At set time points between 0 and 180 min, samples of 3 mL were removed, and the medium was replaced with 3 mL fresh buffer solution (37 °C). The amount of dissolved IND was investigated by UV-Vis spectroscopy at these time points. The observed drug release for the P(VP-co-VA) and PVP containing samples with 50wt% drug loading were normalize to 100% drug release, and drug release for samples with 80wt% drug loading were scaled using the same scaling factor. For

the P1 and P2 containing samples, no normalization was conducted. The data was evaluated using Origin software.

2.11 Dissolution study – non-sink conditions

For supersaturation tests drug loaded extrudates were weighed in equivalents resulting in a total 10 g/L drug concentration in 1 mL phosphate buffer solution (pH = 6.8) (Ph. Eur.) in 1.5 mL Fisherbrand microcentrifuge tubes (Fisher Scientific, Vantaa, Finland). The samples were incubated at 37 °C and mixed at 1100 rpm in a thermomixer (Eppendorf, Hamburg, Germany). At predetermined timepoints between 0 and 30 min, the samples were removed and centrifuged for 2 min at 10000 rpm in a mini centrifuge (Eppendorf, Hamburg, Germany). Afterwards, 10 µL of the supernatant was removed and dissolved in EtOH to determine the drug concentration by UV-Vis spectroscopy.

2.12 Long-term stability study

The samples were stored in a desiccator over silica beads at room temperature. After 1.5 years, DSC thermograms of the samples were measured using the same protocol as described above.

3 Results and Discussion

3.1 Polymer synthesis and characterization

The synthesis of the ABA triblock copolymers, comprising MeOx as block A and BuOx or BuOzi, respectively as block B, was conducted via cationic ring opening polymerization with sequential monomer addition to achieve a block-like polymer architecture as reported previously.[23] Detailed information about the synthesis and polymer analysis can be found elsewhere[20] and in the Supporting Information (Figure S3 – S4, Table S3 – S4). After synthesis, the polymers were analyzed using ^{1}H NMR spectroscopy and SEC and their glass transition temperatures (T_g) were obtained from DSC measurements (Table 1). ^{1}H-NMR analysis shows the presence of all repeat units, and end group analysis gives a molar mass in reasonable agreement with the expected values. The molar mass values obtained from SEC are significantly different from the expected values, which can be attributed to the PMMA calibration standard. The low dispersity clearly suggests a highly living character of the polymerization. In contrast PVP and P(VP-co-VA) show a much higher dispersity as expected for a radical polymerization. Both, pMeOx-pBuOzi-pMeOx (P1) and pMeOx-pBuOx-pMeOx (P2) revealed a single T_g at 50 °C (P1) and 61 °C (P2), respectively. The relatively low T_g compared to PVP K17 (138 °C) and P(VP-co-VA) (103 °C) is potentially beneficial for excipients for hot melt extrusion, in particular for the formulation of heat sensitive drugs (e.g. indomethacin), as the processing temperature can be lowered to prevent possible degradation of the drug.

Table 1. Overview showing the polymer characteristics of the polymers P1, P2, PVP and P(VP-co-VA), including the theoretical molecular weight ($M_{w,\ theo.}$), the molecular weight determined by ^{1}H NMR spectroscopy ($M_{n,\ NMR}$) and SEC ($M_{n,\ SEC}$) and the glass transition temperature determined by DSC (T_g).

	$M_{w,\ theo.}$ [kg mol^{-1}]	$M_{n,\ NMR}$ [kg mol^{-1}]	$M_{n,SEC}$ [kg mol^{-1}]	Đ	T_g [°C]
P1	9.4	8.1	15.3	1.12	50 °C
P2	8.6	8.0	14.7	1.10	61 °C
PVP	7 – 11[a]	n.a.	3.7	2.1	138 °C
P(VP-co-VA)	45 - 70[a]	n.a.	16.9	2.4	103 °C

[a] provided by the manufacturer

3.2 Preparation of drug loaded extrudates

For the custom-synthesized polymers P1 and P2, six different polymer-to-drug ratios were prepared, ranging from 25wt% to 80wt% drug content (Table 2, Supporting Information Tables S5 - S6). For comparison, extrudates of IND and the established excipients PVP and P(VP-co-VA) were prepared with a drug content of 50wt% and 80wt%. To achieve a sufficiently low viscosity for all POx/POzi based samples the extrusion temperature was set to 140 °C in the first heating zone and between 130 and 120 °C in the second and third heating zones, respectively, with minor temperature adjustments depending on the process flow. The extrudates utilizing PVP as polymer excipients were prepared with 135 °C in the first and second heating zones and 140 °C in the third heating zone. For P(VP-co-VA), the process temperature was set to 140 °C in all heating zones. Unexpectedly, the significantly lower T_g of P1 and P2 did not translate into a correspondingly lower processing temperature over PVP and P(VP-co-VA). This was because, unlike for PVP and P(VP-co-VA), the viscosities of P1 and P2 just above their T_g values were still too high for extrusion. On the other hand, due to a sufficiently low viscosity of all polymers at the specified process temperatures, it was possible to keep process temperatures below the melting temperature of IND (T_m = 161 °C, Supporting Information Figure S6), which helps to prevent degradation of the drug. It is important to note that the preparation of ASDs below the T_m of the drug is possible, if the process temperature is above the solubility temperature of the drug in the polymer matrix.[40-41] Detailed information about the process parameter for every sample is listed in the Supporting Information (Table S5 - Table S6).

3.3 Analysis of drug loaded extrudates

Depending on the drug loading, the visual appearance of the polymer-drug extrudates differs significantly (Figure 1, Supporting Information Figure S7). The samples with lower drug loadings have a bright yellow color, are transparent and possess a smooth surface. This was observed up to a drug loading of 60wt% for P1 and P2. Increasing the amount of drug in the sample further to 75wt% or 80wt% results in extrudates with a rough surface and residual heterogeneities, presumably residual crystalline drug particles, which are visible with the naked eye. Similar observations were made for the PVP and P(VP-co-VA) controls — the samples containing 50wt% drug are bright yellow in color and transparent, whereas the samples containing 80wt% drug contained heterogeneities, resulting in opaque samples with a rough surface structure (Supporting Information Figure S7).

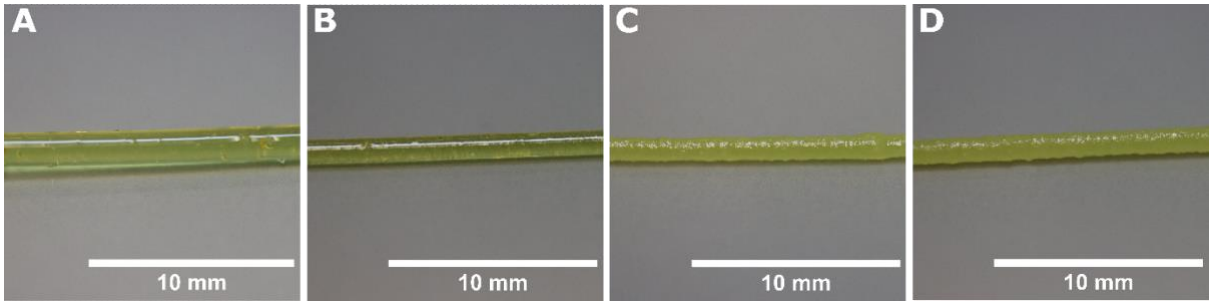

Figure 1. Photographs of the drug loaded extrudates containing P1 and 50wt% (A), 60wt% (B), 75wt% (C) and 80wt% (D) IND, respectively.

The optical observations of the drug loaded extrudates were corroborated by PXRD diffractograms (Figure 2A). After extrusion, the samples exhibit different patterns depending on their drug loading. For the samples containing P1 and a drug loading of 80wt%, the characteristic Bragg peaks of γ-IND[42] are still present, while the diffuse halo is barely visible, indicating high residual crystallinity of the drug. Upon decreasing the drug loading to 75wt% and below, these characteristic peaks are no longer observed, suggesting successful preparation of ASDs. It is important to note, however, that PXRD is a bulk analysis method and, at the same time, as drug loading decreases the background noise increases relative to the drug loading. These factors make it challenging to rule out residual trace crystallinity. The ASD samples with P2, PVP and P(VP-co-VA) (Supporting Information Figure S8 – S10) as excipients show an essentially identical behavior. Only the extrudates with the highest drug loading of 80wt% for all three polymers exhibit the characteristic Bragg peaks indicating the presence of γ-IND. Successful ASD preparation with various drug loadings and different preparation methods is well documented for both PVP and P(VP-co-VA).[43] With IND as a model drug, spray dried ASDs with up to 85wt% and 70wt% drug loading were reported for PVP and P(VP-co-VA), respectively.[44-45]

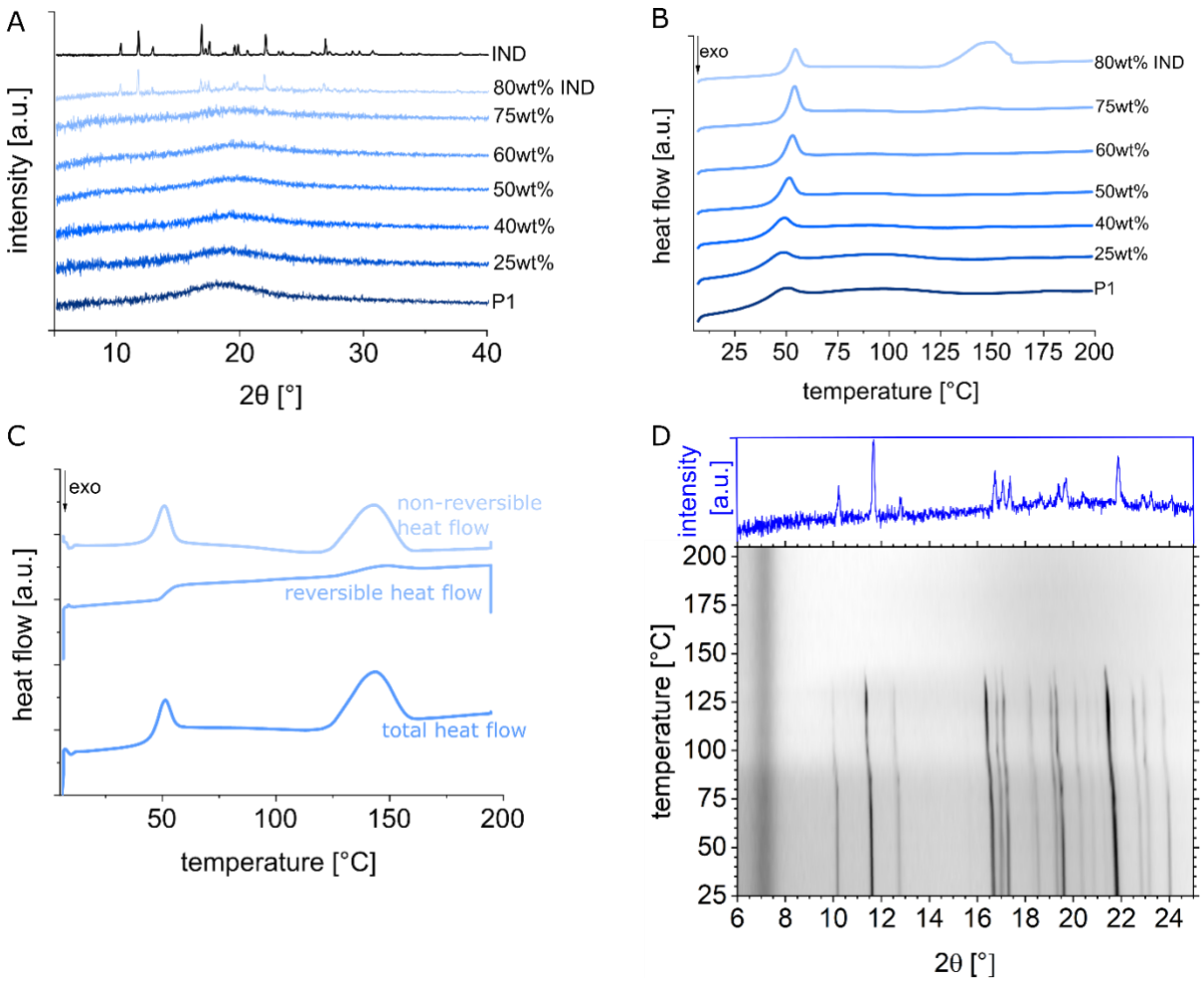

Figure 2. A) PXRD diffractograms and B) DSC thermograms of the extrudates with polymer P1 and IND at different polymer to drug ratios. Further characterization of the extrudate containing 20wt% P1 and 80wt% IND by C) modulated DSC (mDSC) and D) PXRD at variable temperature with the room-temperature diffractogram of pure γ-IND (in blue) as a control.

DSC was used to study the thermal properties of the extrudates. As the solubility of the drug in the polymer matrix changes with increasing temperature, only the first heating cycle of the measurements was considered. For P1, interestingly, extrusion of the pure polymer alone changed its T_g. Before extrusion, the T_g of the polymer was 50 °C (Table 1), while after extrusion, it dropped to 45 °C (Figure 2B), indicating the influence the processing method can have on the glass transition of an amorphous system. It is unlikely the lower T_g is due to degradation during HME, as SEC measurements before and after the extrusion process resulted in identical elugrams (Supporting Information Figure S11).

By comparing the thermograms and thermal events of the ASDs containing P1 (Figure 2B, Table 2) it can be seen that all dispersions for this polymer exhibit a single T_g. The T_g values are between 43 °C and 49 °C, and therefore are between those of the neat polymer before extrusion and neat IND (43°C).

Table 2. Glass transition temperatures (T_g) for all prepared extrudates with different polymer-to-drug ratios.

polymer/drug ratio [wt%]	T_g [°C]			
	P1	P2	PVP	P(VP-co-VA)
100:0	45	61	138	103
75:25	43	55	-	-
60:40	45	55	-	-
50:50	47	56	79	72
40:60	48	56	-	-
25:75	48	56	-	-
20:80	49	53	56	53

In addition to the T_g, a broad endothermic transition can be observed in the thermogram comprising the highest drug loading (80wt% drug), which appears not at the melting temperature of IND (160 °C) but at ca. 140 °C. This is presumably due to the increasing solubility of the drug in the polymer matrix with increasing temperature, and thus dissolution of the remaining crystallites, further evidenced by the absence of a subsequent melting peak. Such behavior with IND in POx/POzi based ASDs has previously been reported.[19]

To gain more insight into this transition with P1 and to confirm our hypothesis, modulated DSC (Figure 2C) and variable temperature PXRD (Figure 2D) were performed. Usually, melting of the residual crystallinity in the sample manifests as a relatively well defined endothermic peak in a reversible heat flow thermogram [48], while here, only a very broad transition starting at 140 °C is observed, as expected for a gradual dissolution. Variable temperature PXRD diffractograms ranging from 25 °C to 200 °C (Figure 2D) reveal that increasing temperature leads to a gradual shift of the diffraction peaks in the crystal pattern to lower angles, consistent with thermally-induced crystal lattice expansion, followed by weakening of the signal starting around 135 °C and their disappearance at around 145 °C, consistent with dissolution. This corroborated our hypothesis that the solubility of the drug in the polymer matrix is increasing with increasing temperature with the drug fully dissolving in the polymer matrix prior to the melting of IND. This supersaturated glass solution is apparently kinetically stable for a certain amount of time, as there was no recrystallization of the drug observed when heated again for second and third heating cycles (data not shown). The thermograms only displayed one T_g, at 49 °C (P1 with 80wt% IND), with no other thermal events, indicating maintenance of a single amorphous polymer-drug phase.

The same general behavior is also observed in the thermograms of P2 and IND (Supporting Information Figure S8). The T_g, including enthalpic relaxation, was observed between 53 °C and 61 °C, depending on the drug loading. In the samples exhibiting residual crystalline

particles upon visual inspection (75wt% and 80wt% drug loading) a broad endothermic transition starting at approximately 125 °C, consistent with dissolution of these crystals in the polymer is observed, while a clear endothermic peak, suggestive of IND melting, is absent.

The extrudates of PVP or P(VP-co-VA) and IND exhibited similar thermal behavior, to POx/POzi (Supporting Information Figure S9 – S10). The T_gs of the extrudates were observed between 53 °C and 79 °C, depending on the polymer and drug content. As with P1 and P2, the T_g decreased with increasing drug content due to the plasticizing effect of IND.[36] However, for these two polymers, the difference of the T_g for the two different drug loadings (50 and 80wt%) is about 20 °C, due to the much higher T_gs of the polymers themselves (T_g(P(VP-co-VA) = 103 °C and T_g(PVP) = 138 °C). In contrast, for P1 and P2, the T_g of the pure polymers and drug differ only by approximately 10 °C, resulting in a minor difference in T_g depending on drug loading. Additionally, the samples containing PVP or P(VP-co-VA) show a broad endothermic transition between 130 °C and 180 °C at 80wt% drug loading, presumably due to drug dissolution in the polymer, as discussed for P1 and P2. Furthermore, none of the samples showing initial residual crystallinity in the first heating exhibited recrystallization of the drug upon subsequent heating cycles (data not shown). This suggests that for longer residence times or higher temperature during extrusion fully amorphous ASDs could be obtained even at 80wt% drug loading, albeit at the risk of drug degradation and/or polymer degradation.

3.4 ^{13}C CPMAS NMR spectroscopy

To further assess the interaction between polymer and drug, including hydrogen bonding, solid state ^{13}C NMR spectroscopy was conducted. First, ASDs containing the polymer P1 with different polymer-drug ratios, as well as the plain polymer, crystalline and amorphous IND, were compared (Figure 3). Depending on the solid-state form of the drug, pronounced differences in the spectra are visible. The γ-IND polymorph shows narrow lines with one peak for each carbon atom. This indicates that there is one molecule in the asymmetric unit of the crystal lattice, which is consistent with the known crystal structure of γ-IND.[49-50] This polymorph consists of cyclic dimers formed via hydrogen bonding between the carboxylic acid groups of two IND molecules, which gives rise to the peak at 180 ppm (assigned as signal 1 in Figure 3B). Importantly, Strachan et al. reported that such dimers are also predominant in amorphous IND, as evidenced by infrared and Raman spectroscopies.[51] The other peak in the carbonyl region, at 167 ppm (signal 2), corresponds to the amide group, which is not involved in hydrogen bonding in the γ-polymorph.[42] Compared to the spectrum of the crystalline form, the spectrum of the amorphous form shows broader peaks with an additional shoulder next to the peak at 167 ppm, probably resulting from a combination of conformations

and intermolecular bonding present in α- and γ-IND.[49] Besides the carboxylic acid dimer, hydrogen bonded carboxylic acid-amide complexes are present in the α-polymorph. Deconvolution of the CPMAS ^{13}C spectrum of amorphous IND by Yuan et al. showed, that besides the aforementioned conformations, free carboxylic acid and hydrogen bonded carboxylic acid chain conformations are present as well. [49]

The spectrum of P1 shows broad signals with one prominent peak at 172 ppm (signal 4 in Figure 3B), attributed to the amide group of the POx/POzi repeating units. This signal appears between signals 1 and 2 of γ-IND, and it is overlapping with the additional shoulder of signal 2 in amorphous IND. In the spectra of samples containing both P1 and IND, signal 1 is absent up to an IND loading of 60wt%. In contrast, starting from 75wt% IND, signal 1 is again visible. This indicates that the H-bonding capacity of P1 with IND is somewhat saturated at this point, leading to the formation of IND carboxylic acid dimers. Similarly, signal 2 is not observed below a drug loading of 50wt% but appears as a shoulder at lower ppm values (172 ppm) above 50wt%, with its intensity increasing with increasing drug loading.

A similar trend as described above for P1 can be observed in the samples comprising P2 and IND (Supporting Information Figure S12). At 80wt% drug, signals 1 and 2 are clearly observable, while at 75wt% signal 1 disappears. Signal 2, on the other hand, remains visible as a shoulder of signal 4. With a further decrease in the drug loading, neither signal 1 nor 2 are observed in the spectra.

Yuan et al. investigated hydrogen bonding interactions of IND in amorphous solid dispersions with PVP and P(VP-co-VA).[49] Besides showing the existence of several interactions of the carboxylic acid moiety of IND in the ASD, including the carboxylic acid hydrogen of IND binding to the PVP carbonyl and/or vinyl acetate carbonyl of P(VP-co-VA), they showed that with increasing polymer content, the signal displaying the IND carboxylic acid dimers decreases, which is in line with our observations for the IND-P1 / IND-P2 ASDs (Figure 3, Supporting Information Figure S11). At the same time, the signal attributed to the carboxylic acid-amide complex increases and gradually dominates the spectrum. For the samples containing P1 or P2 this manifests as the observed shoulder of signal 4 at approximately 172 ppm. Additionally, Yuan et al. observed that both polymers, PVP and P(VP-co-VA), in general showed the same behavior regarding hydrogen bonding with IND. However, the hydrogen bond accepting capability of the polymers differed. Due to the lower content of tertiary amides in P(VP-co-VA) compared to PVP, fewer carboxylic acid – amide complexes can form in the ASD, which is in line with the observations that the signal attributed to the IND carboxylic acid dimer is more intense for P(VP-co-VA) than for PVP in ASDs with the same drug loading.[49]

As indomethacin dimers with cyclic hydrogen bonding between the carboxylic acid moieties are present in both IND polymorphs, α- and γ-, carboxylic acid dimer formation is probably a critical step in the crystallization process from drug-polymer mixes.[42] It should be noted that the dimers described by Strachan et al. in amorphous IND[51] might serve as nucleation points for crystallization. Also Yuan et al. hypothesized that the absence of drug-drug dimers or the inhibition of dimer formation in an ASD due to polymer-drug hydrogen bonding, could effectively inhibit the recrystallization of the drug in the ASD at room temperature and therefore benefit the stability of the amorphous form of the drug.[49] A similar hypothesis regarding the stability of polymer-drug mixtures between PVP and IND was suggested by Matsumoto et al. The authors argue that the interaction between the carboxylic acid group of the drug and the amide carbonyl of the polymer inhibits the formation of carboxylic acid dimers and therefore the recrystallization of the drug from the ASD.[52]

In the current study, the presence or absence of signal 1 at 180 ppm, and therefore the presence or absence of the IND carboxylic acid dimers, can be used as an indicator of IND crystallinity and possibly, the propensity of an ASD to suppress recrystallization. Transferring this to the ASDs prepared with P1 and P2, samples with 60wt% IND for P1 and 75wt% for P2 (or less) should be highly resistant against crystallization over time. To test this hypothesis, thermograms of the extrudates containing IND and P1 or P2, respectively, were recorded 1.5 years after the preparation of the samples (Supporting Information Figure S13). None of the samples showed signs of crystallization. Only one sample (50wt% drug loading, P2) showed a shift in T_g and an additional broad endothermic transition between 60 and 125 °C, which we tentatively attribute to water uptake, as the samples were only stored in a desiccator over silica beads (without regeneration over time), but not otherwise protected from humidity. Overall, NMR spectroscopy clearly corroborates findings from DSC and PXRD, showing that P1 and P2 are highly effective crystallization inhibitors for IND, similar to PVP and P(VP-co-VA).

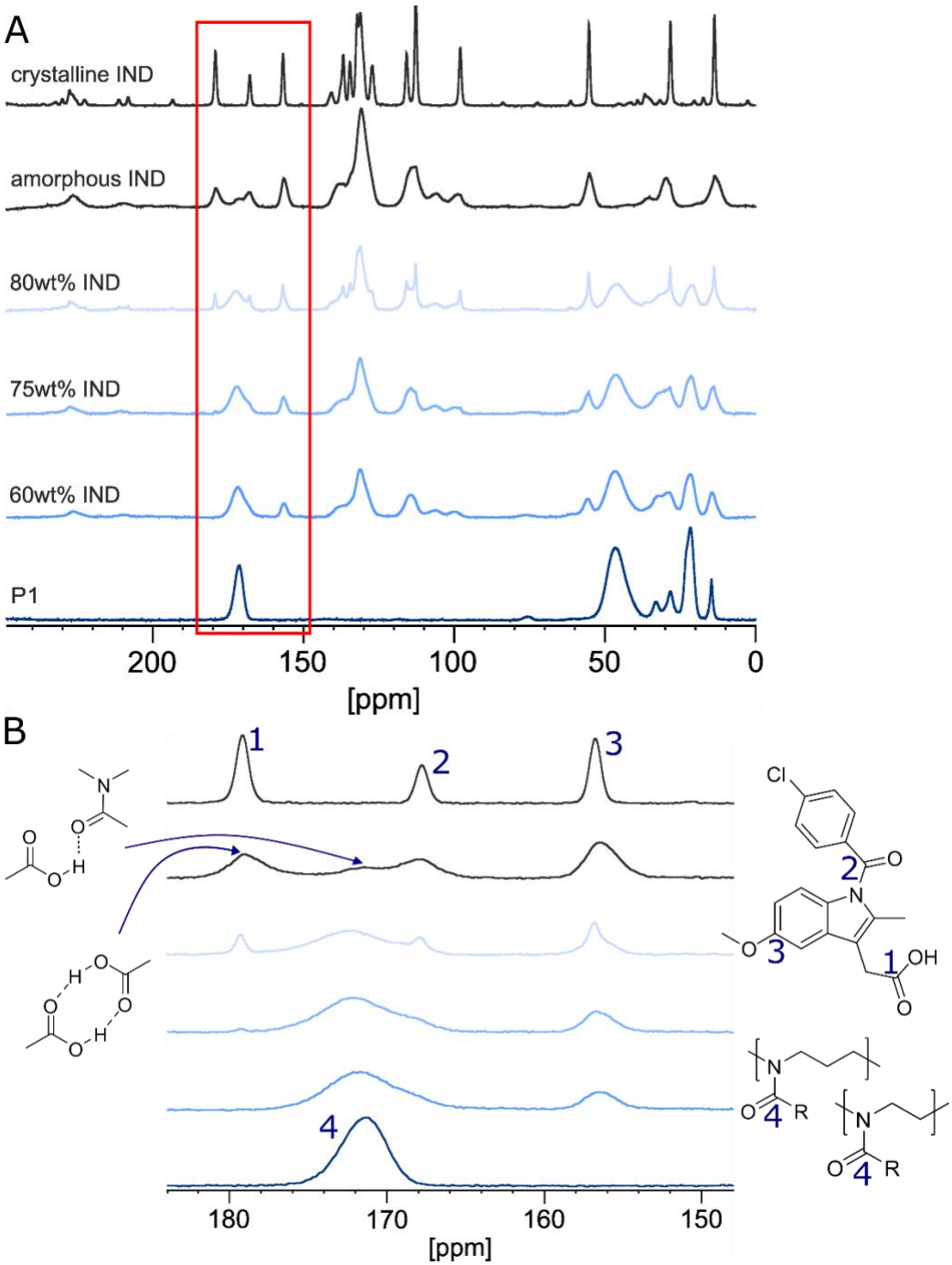

Figure 3. (A) ^{13}C CPMAS NMR spectra of P1, crystalline and amorphous IND and three P1-drug mixtures (60wt%, 75wt% and 80wt% IND loading) and (B) a close-up view between 184 and 148 ppm of the marked area (red box in A) with assignment of the most important signals. Signals 1, 2 and 3 correspond to IND, signal 4 is attributed to the amide carbon atom in the 2-oxazoline and 2-oxazine polymer sidechain.

3.5 Dissolution testing

To assess differences in the dissolution profiles of all four excipients for ASDs containing 50wt% and 80wt% drug, respectively, dissolution experiments (under sink conditions) were conducted with the prepared extrudates (Figure 4). Irrespective of the polymer used, samples

containing 50wt% drug loading exhibited a faster relative dissolution rate than samples containing 80wt% drug. At 50wt% drug loading, IND in P1 and P2 dissolved completely within 30 min, whereas IND in the extrudates containing PVP and P(VP-co-VA) dissolved within 10 and 15 min, respectively. The rather large error bars obtained for P2 at 50wt% may be due to incomplete mixing of the drug within the ASD. A similar trend between polymers regarding the drug dissolution rate can be observed for the samples containing 80wt% IND. The drug loaded samples containing P1 and P2 dissolved somewhat more slowly than the ASDs prepared with PVP and P(VP-co-VA), but the difference between the excipients is less pronounced and none of the samples reached a plateau with respect to drug release within the investigated time. The difference between the sets of ASDs at different drug loading can be largely explained by the differences in the solid-state form of the drug. At 50wt% drug loading, all ASDs are fully amorphous, whereas at 80wt% drug loading, a significant amount of residual crystalline drug is present. As amorphous IND has a higher aqueous solubility and consequently dissolution rate compared to its crystalline form, due to its higher free energy[53], the corresponding fully amorphous ASDs show faster dissolution compared to the partially crystalline ones. An additional factor likely contributing to the higher drug release at 50wt% drug loading, is the larger influence of the highly soluble polymer at the 50wt% compared to 80wt% drug loading.

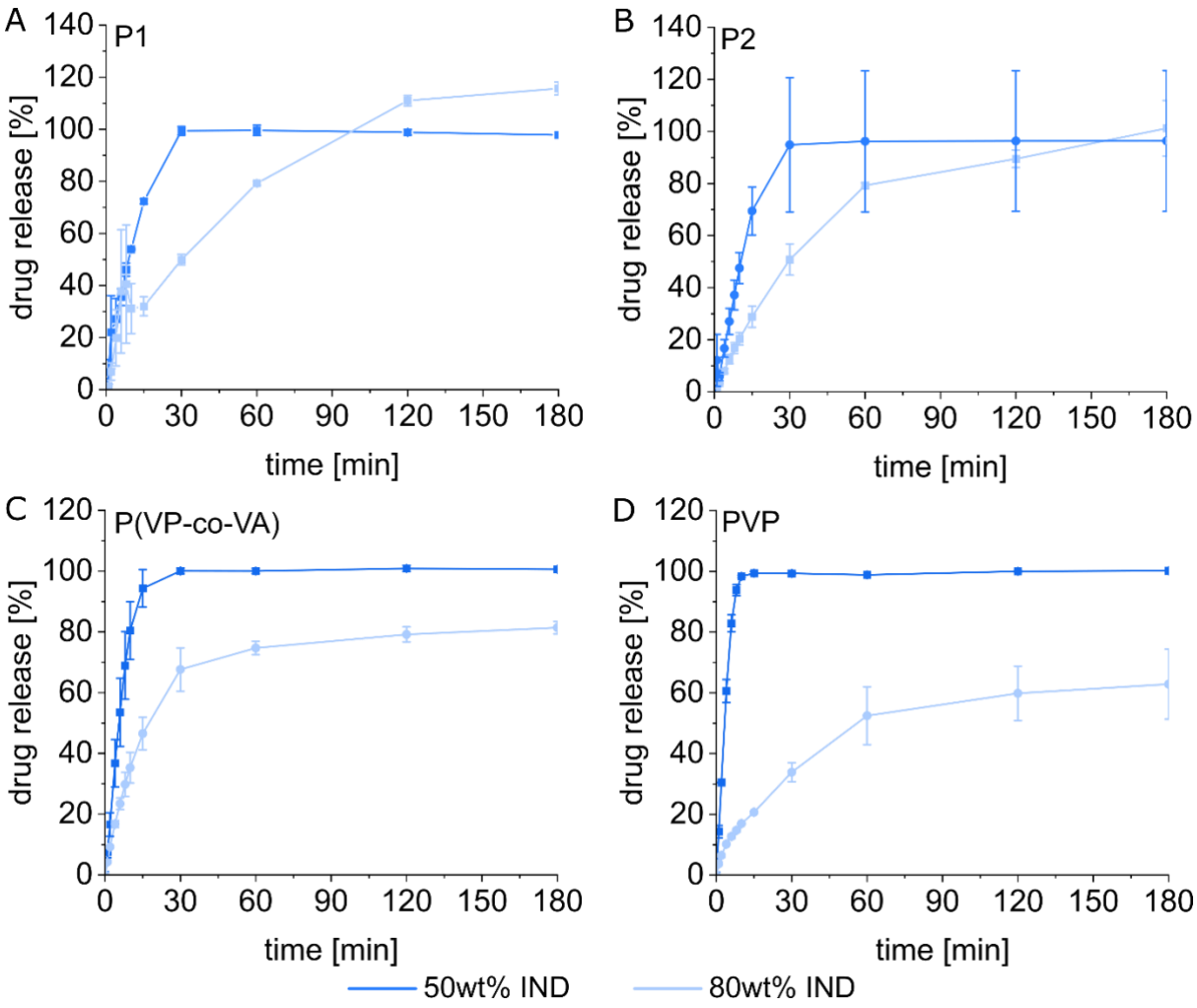

Figure 4. Dissolution profiles under sink conditions (in PBS, pH = 6.8) of P1 (A), P2 (B), P(VP-co-VA) (C) and PVP (D) extrudates, respectively, containing 50wt% and 80wt% drug loading. The profiles of 50wt% drug loading of P(VP-co-VA) and PVP were scaled to 100% drug release, and profiles for 80wt% drug loading were scaled accordingly.

In addition to dissolution under sink conditions, dissolution tests under non-sink conditions (supersaturation) of all four polymer samples containing 50wt% and 80wt% IND loading were performed (Figure 5). In these experiments, the maximal drug concentration in all experiments was set to 10 g/L, which is significantly above the solubility of γ-IND (1.65 g/L, confirmed in-house). The P(VP-co-VA) sample with 50wt% drug loading fully dissolved within the first 20 min, resulting in a maximal drug concentration of 10 g/L. Due to partial precipitation of the drug thereafter, the drug concentration decreased to 7.5 g/L, at which it appeared to stabilize. A similar trend can be observed for P1 with 50wt% drug loading. Within the first 20 min a maximal drug concentration of 8 g/L was reached, followed by partial precipitation, resulting in 5.7 g/L IND concentration after 180 min. The P1 and P(VP-co-VA) extrudates containing 80wt% drug showed a slower drug dissolution over 60 min, until maximal drug concentrations of 5.5 g/L and 5.9 g/L were reached, respectively. The use of P2 and PVP as excipients in the ASD resulted in a maximal dissolution of approximately 5 g/L and 4 g/L IND, respectively. Similar

as for P1 and P(VP-co-VA), the initial dissolution is faster at 50wt% drug loading for these two excipients, while the maximal IND concentration is very similar irrespective of the drug loading.

Summarizing the results from both dissolution experiments, the amount of drug in the ASDs determines the relative dissolution rates for all tested polymers; with lower drug loading leading to faster dissolution. In contrast to what we expected, the ability of P1 and P2 to form micelles does not lead to higher maximum drug concentrations or improved supersaturation compared to PVP or P(VP-co-VA) in the current non-sink dissolution setup. However, this likely depends on the employed drug and should not be generalized. For IND, ionization of the drug in the buffer, crystallization and possibly also amorphous phase separation are also expected to influence drug release, and these types of behaviors strongly depend on the molecular properties of the drug and dissolution medium. IND in pH 6.8 buffer may in fact have not been an ideal choice to highlight the potential of P1 or P2 to achieve high and sustained supersaturation of poorly soluble drugs. Firstly, the pH of the dissolution medium would have promoted ionization and therefore dissolution of IND, regardless of the polymer. Secondly, both polymers presented only as intermediate solubilizers for IND from drug loaded thin films.[56-57] However, these polymers have been found to be excellent solubilizers for several other drugs including various taxanes[29, 31], curcumin[23], clotrimazole[29] and vismodegib[29, 58], and we hypothesize that for these drugs, the performance of P1 and P2 as ASD excipients could outperform established excipients such as PVP and P(VP-co-VA), which will be investigated in future work.

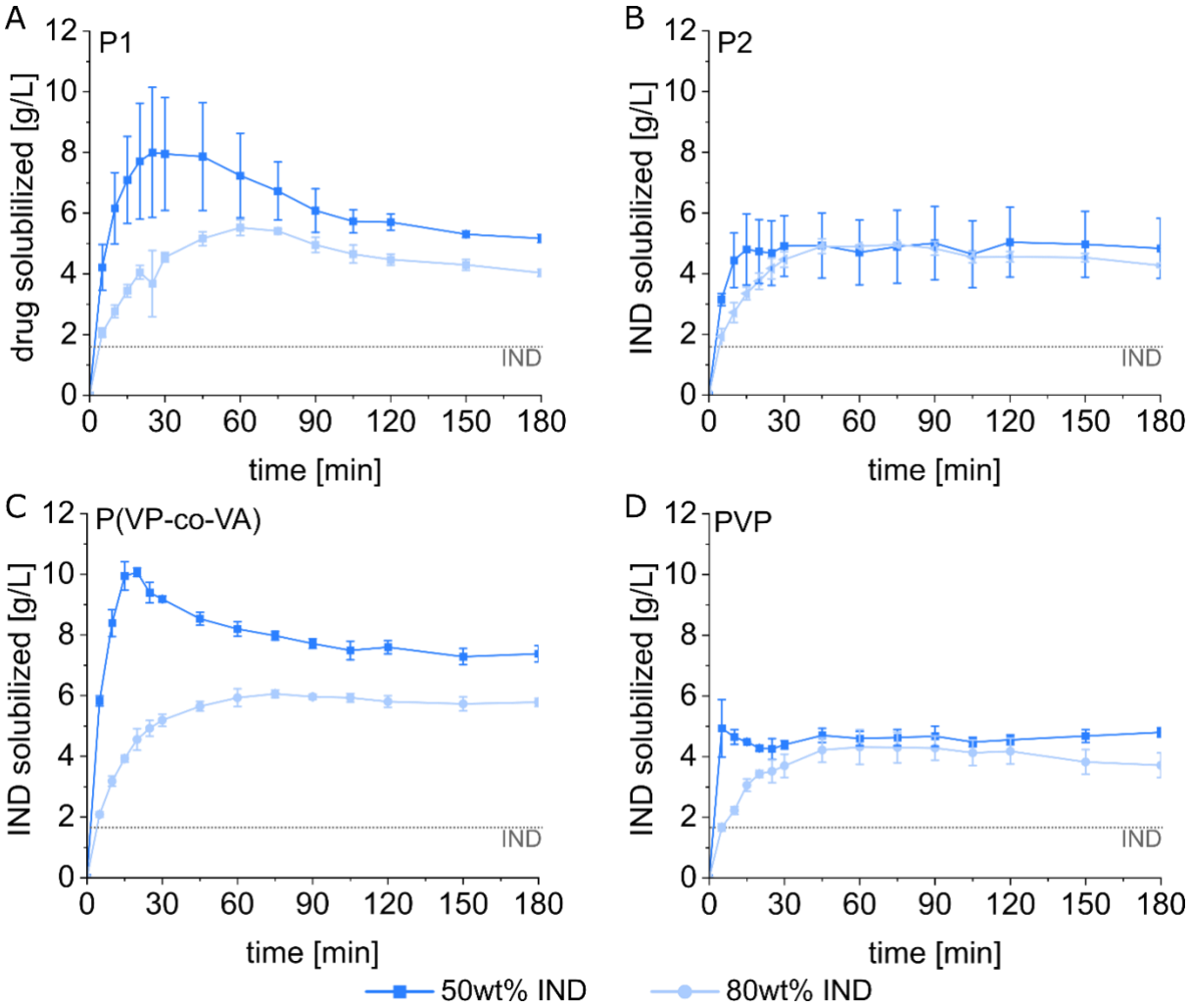

Figure 5. Non-sink dissolution test (PBS, pH = 6.8) of extrudates containing IND as model drug and P1 (A), P2 (B), P(VP-co-VA) (C) and PVP (D), respectively. The drug concentration was kept constant at 10 g/L for each sample. The maximal solubility achieved for γ-IND is added as a grey dashed line (1.65 g/L).

4 Conclusion

The performance of POx and POzi based polymers as crystallization inhibiting excipients in ASDs at high drug loading was compared to the industrially established polymers PVP and P(VP-co-VA). To this end, two amphiphilic ABA triblock copolymers, pMeOx-pBuOzi-pMeOx (P1) and pMeOx-pBuOx-pMeOx (P2), were synthesized and used as excipients in the preparation of ASDs of IND via hot melt extrusion at different drug loadings (from 25 to 80wt%). Extrudates containing the structurally similar PVP and P(VP-co-VA) were prepared with IND loadings of 50 and 80wt%. For the extrudates containing P1 and P2, DSC and PXRD measurements indicate that the samples are fully amorphous up to a drug loading of 75wt%, but analysis of ^{13}C CPMAS NMR data indicates the presence of IND carboxylic acid dimers at 75wt% drug loading in the case of P1. This suggests saturation of the H-bonding capacity

between polymer and drug. Below 75wt% drug loading the ^{13}C CPMAS NMR data indicated that the samples are amorphous regardless of the polymer used. Even after 1.5 years of storage, no further recrystallization was detected. When using PVP and P(VP-co-VA), residual crystallinity was detected only at a drug loading of 80wt% by DSC and PXRD. Furthermore, differences depending on the used polymer and drug content in the ASD are observed in the dissolution profile of the extrudates. The samples with lower drug loading generally dissolved faster. Comparing excipients, ASD based on PVP and P(VP-co-VA) dissolved faster than the samples made using P1 and P2. The difference in dissolution rate was observed under non-sink dissolution experiments as well. Here, the ASD comprising P1 and P(VP-co-VA) as excipients achieve higher maximal drug concentration compared to the other two polymers.

This study introduces new polymers for use in ASDs prepared via hot melt extrusion. Using IND as a model drug, these polymers provided drug loading capacity and dissolution kinetics comparable to the well-known excipients PVP and P(VP-co-VA). Given the broader advantages of a having a wider range of polymers available for formulating ASDs, the potential of POx and POzi based polymers should be further evaluated for drugs for which these polymers are known to be good solubilizers, with an additional focus on the effects of dissolution medium on drug release.

Acknowledgements

The authors acknowledge the financial support by the Academy of Finland (Grant no. 337660 and Grant no. 342983). The authors thank Mikko Heikkilä and Heikki Räikkönen for their assistance in PXRD measurements, Sami-Pekka Hirvonen for SEC measurements, and Alexandra Correia for technical assistance. Furthermore, the synthesis of polymer P2 by Mengshi Yang and Christian May is appreciated.

Conflict of Interest

The authors declare the following potential conflicts of interest(s): R.L. is listed as inventor on patents and patent applications pertinent to some materials discussed in this contribution and is co-founder of DelAQUA Pharmaceuticals, intending to commercialize poly(2-oxazoline) based drug formulations.

CRediT authorship contribution statement

L. Keßler: Conceptualization, Investigation, Visualization, Data curation, Writing – original draft; R. Mishra: Conceptualization, Investigation, Writing – review & editing; M. Lammens, S.

Hietala: Investigation, Writing – review & editing; T. Rades, A. Juppo, T. Laaksonen: Funding acquisition, Writing – review & editing; B. van Veen, C. Strachan: Conceptualization, Funding acquisition, Writing – review & editing, Supervision. R. Luxenhofer: Conceptualization, Funding acquisition, Writing – review & editing, Writing – original draft, Supervision. All authors have read and agreed to the published version of the manuscript.

References

[1] S. Baghel, H. Cathcart, N. J. O'Reilly Polymeric Amorphous Solid Dispersions: A Review of Amorphization, Crystallization, Stabilization, Solid-State Characterization, and Aqueous Solubilization of Biopharmaceutical Classification System Class II Drugs *J Pharm Sci* **2016**, *105*, 2527-2544.

[2] M. Beneš, T. Pekárek, J. Beránek, J. Havlíček, L. Krejčík, M. Šimek, M. Tkadlecová, P. Doležal Methods for the preparation of amorphous solid dispersions – A comparative study *J Drug Deliv Sci Technol* **2017**, *38*, 125-134.

[3] P. Pandi, R. Bulusu, N. Kommineni, W. Khan, M. Singh Amorphous solid dispersions: An update for preparation, characterization, mechanism on bioavailability, stability, regulatory considerations and marketed products *Int J Pharm* **2020**, *586*, 119560-119587.

[4] A. B. Anane-Adjei, E. Jacobs, S. C. Nash, S. Askin, R. Soundararajan, M. Kyobula, J. Booth, A. Campbell Amorphous solid dispersions: Utilization and challenges in preclinical drug development within AstraZeneca *Int J Pharm* **2022**, *614*, 121387-121402.

[5] A. Singh, Z. A. Worku, G. Van den Mooter Oral formulation strategies to improve solubility of poorly water-soluble drugs *Expert Opin Drug Deliv* **2011**, *8*, 1361-1378.

[6] G. Van den Mooter, M. Wuyts, N. Blaton, R. Busson, P. Grobet, P. Augustijns, R. Kinget Physical stabilisation of amorphous ketoconazole in solid dispersions with polyvinylpyrrolidone K25 *Eur J Pharm Sci* **2001**, *12*, 261-269.

[7] U. S. Kestur, L. S. Taylor Role of polymer chemistry in influencing crystal growth rates from amorphous felodipine *CrystEngComm* **2010**, *12*, 2390-2397.

[8] T. Xie, L. S. Taylor Dissolution Performance of High Drug Loading Celecoxib Amorphous Solid Dispersions Formulated with Polymer Combinations *Pharm Res* **2016**, *33*, 739-750.

[9] S. V. Bhujbal, B. Mitra, U. Jain, Y. Gong, A. Agrawal, S. Karki, L. S. Taylor, S. Kumar, Q. Tony Zhou Pharmaceutical amorphous solid dispersion: A review of manufacturing strategies *Acta Pharm Sin B* **2021**, *11*, 2505-2536.

[10] A. Alzahrani, D. Nyavanandi, P. Mandati, A. A. A. Youssef, S. Narala, S. Bandari, M. Repka A systematic and robust assessment of hot-melt extrusion-based amorphous solid dispersions: Theoretical prediction to practical implementation *Int J Pharm* **2022**, *624*, 121951-121973.

[11] H. Wu, Y. Liu, T. Ci, X. Ke Application of HPMC HME polymer as hot melt extrusion carrier in carbamazepine solid dispersion *Drug Dev Ind Pharm* **2020**, *46*, 1911-1918.

[12] R. Svoboda, M. Nevyhostena, J. Machackova, J. Vaculik, K. Knotkova, M. Chromcikova, A. Komersova Thermal degradation of Affinisol HPMC: Optimum Processing Temperatures for Hot Melt Extrusion and 3D Printing *Pharm Res* **2023**, *40*, 2253-2268.

[13] A. Butreddy, S. Sarabu, M. Almutairi, S. Ajjarapu, P. Kolimi, S. Bandari, M. A. Repka Hot-melt extruded hydroxypropyl methylcellulose acetate succinate based amorphous solid dispersions: Impact of polymeric combinations on supersaturation kinetics and dissolution performance *Int J Pharm* **2022**, *615*, 121471-121484.

[14] J. T. Morott, M. Pimparade, J. B. Park, C. P. Worley, S. Majumdar, Z. Lian, E. Pinto, Y. Bi, T. Durig, M. A. Repka The effects of screw configuration and polymeric carriers on hot-melt extruded taste-masked formulations incorporated into orally disintegrating tablets *J Pharm Sci* **2015**, *104*, 124-134.

[15] A. Agrawal, M. Dudhedia, W. Deng, K. Shepard, L. Zhong, E. Povilaitis, E. Zimny Development of Tablet Formulation of Amorphous Solid Dispersions Prepared by Hot Melt Extrusion Using Quality by Design Approach *AAPS PharmSciTech* **2016**, *17*, 214-232.
[16] M. Darwich, V. Mohylyuk, K. Kolter, R. Bodmeier, A. Dashevskiy Enhancement of itraconazole solubility and release by hot-melt extrusion with Soluplus® *J Drug Deliv Sci Technol* **2023**, *81*, 104280-104286.
[17] S. S. Gupta, T. Parikh, A. K. Meena, N. Mahajan, I. Vitez, A. T. M. Serajuddin Effect of carbamazepine on viscoelastic properties and hot melt extrudability of Soluplus® *Int J Pharm* **2015**, *478*, 232-239.
[18] S. Feng, S. Bandari, M. A. Repka Investigation of poly(2-ethyl-2-oxazoline) as a novel extended release polymer for hot-melt extrusion paired with fused deposition modeling 3D printing *J Drug Deliv Sci Technol* **2022**, *74*, 103558-103567.
[19] L. Keßler, Z. Mirzaei, J. C. Kade, R. Luxenhofer Highly Porous and Drug-Loaded Amorphous Solid Dispersion Microfiber Scaffolds of Indomethacin Prepared by Melt Electrowriting *ACS Appl Polym Mater* **2023**, *5*, 913-922.
[20] M. M. Lübtow, M. S. Haider, M. Kirsch, S. Klisch, R. Luxenhofer Like Dissolves Like? A Comprehensive Evaluation of Partial Solubility Parameters to Predict Polymer-Drug Compatibility in Ultrahigh Drug-Loaded Polymer Micelles *Biomacromolecules* **2019**, *20*, 3041-3056.
[21] M. M. Lübtow, L. Kessler, A. Appelt-Menzel, T. Lorson, N. Gangloff, M. Kirsch, S. Dahms, R. Luxenhofer More Is Sometimes Less: Curcumin and Paclitaxel Formulations Using Poly(2-oxazoline) and Poly(2-oxazine)-Based Amphiphiles Bearing Linear and Branched C9 Side Chains *Macromol Biosci* **2018**, *18*, 1800155-1800171.
[22] M. S. Haider, M. M. Lübtow, S. Endres, S. Forster, V. J. Flegler, B. Bottcher, V. Aseyev, A. C. Poppler, R. Luxenhofer Think Beyond the Core: Impact of the Hydrophilic Corona on Drug Solubilization Using Polymer Micelles *ACS Appl Mater Interfaces* **2020**, *12*, 24531-24543.
[23] M. M. Lübtow, L. Hahn, M. S. Haider, R. Luxenhofer Drug Specificity, Synergy and Antagonism in Ultrahigh Capacity Poly(2-oxazoline)/Poly(2-oxazine) based Formulations *J Am Chem Soc* **2017**, *139*, 10980-10983.
[24] Z. He, X. Wan, A. Schulz, H. Bludau, M. A. Dobrovolskaia, S. T. Stern, S. A. Montgomery, H. Yuan, Z. Li, D. Alakhova, M. Sokolsky, D. B. Darr, C. M. Perou, R. Jordan, R. Luxenhofer, A. V. Kabanov A high capacity polymeric micelle of paclitaxel: Implication of high dose drug therapy to safety and in vivo anti-cancer activity *Biomater* **2016**, *101*, 296-309.
[25] M. M. Lübtow, S. Oerter, S. Quader, E. Jeanclos, A. Cubukova, M. Krafft, M. S. Haider, C. Schulte, L. Meier, M. Rist, O. Sampetrean, H. Kinoh, A. Gohla, K. Kataoka, A. Appelt-Menzel, R. Luxenhofer In Vitro Blood-Brain Barrier Permeability and Cytotoxicity of an Atorvastatin-Loaded Nanoformulation Against Glioblastoma in 2D and 3D Models *Mol Pharm* **2020**, *17*, 1835-1847.
[26] N. Vinod, D. Hwang, S. C. Fussell, T. C. Owens, O. C. Tofade, T. S. Benefield, S. Copling, J. D. Ramsey, P. D. Rädler, H. M. Atkins, E. E. Livingston, J. A. Ezzell, M. Sokolsky-Papkov, H. Yuan, C. M. Perou, A. V. Kabanov Combination of polymeric micelle formulation of TGFβ receptor inhibitors and paclitaxel produces consistent response across different mouse models of Triple-negative breast cancer *Bioeng Transl Med* **2024**, *e10681*.
[27] D. Hwang, N. Vinod, S. L. Skoczen, J. D. Ramsey, K. S. Snapp, S. A. Montgomery, M. Wang, C. Lim, J. E. Frank, M. Sokolsky-Papkov, Z. Li, H. Yuan, S. T. Stern, A. V. Kabanov Bioequivalence assessment of high-capacity polymeric micelle nanoformulation of paclitaxel and Abraxane(R) in rodent and non-human primate models using a stable isotope tracer assay *Biomater* **2021**, *278*, 121140-121150.
[28] C. Lim, D. Hwang, M. Yazdimamaghani, H. M. Atkins, H. Hyun, Y. Shin, J. D. Ramsey, P. D. Radler, K. R. Mott, C. M. Perou, M. Sokolsky-Papkov, A. V. Kabanov High-Dose Paclitaxel and its

Combination with CSF1R Inhibitor in Polymeric Micelles for Chemoimmunotherapy of Triple Negative Breast Cancer *Nano Today* **2023**, *51*, 101884-101898.
[29] M. S. Haider, R. Luxenhofer Development of Poly (2-oxazoline) s and poly (2-oxazine) s based formulation library and estimation of polymer/drug compatibility *ChemRxiv* **2022**.
[30] J. D. Ramsey, I. E. Stewart, E. A. Madden, C. Lim, D. Hwang, M. T. Heise, A. J. Hickey, A. V. Kabanov Nanoformulated Remdesivir with Extremely Low Content of Poly(2-oxazoline)-Based Stabilizer for Aerosol Treatment of COVID-19 *Macromol Biosci* **2022**, *22*, 2200056-2200067.
[31] R. Luxenhofer, A. Schulz, C. Roques, S. Li, T. K. Bronich, E. V. Batrakova, R. Jordan, A. V. Kabanov Doubly amphiphilic poly(2-oxazoline)s as high-capacity delivery systems for hydrophobic drugs *Biomater* **2010**, *31*, 4972-4979.
[32] C. D'Amico, A. L. Ziegler, M. Kemell, G. Molinaro, R. Luxenhofer, H. A. Santos Self-Nanoformulating Poly(2-oxazoline) and Poly(2-oxazine) Copolymers Based Amorphous Solid Dispersions as Microneedle Patch: A Formulation Study *Ad MaterTechnol* **2024**, 2400766.
[33] O. Sedlacek, V. Bardoula, E. Vuorimaa-Laukkanen, L. Gedda, K. Edwards, A. Radulescu, G. A. Mun, Y. Guo, J. Zhou, H. Zhang, V. Nardello-Rataj, S. Filippov, R. Hoogenboom Influence of Chain Length of Gradient and Block Copoly(2-oxazoline)s on Self-Assembly and Drug Encapsulation *Small* **2022**, *18*, 2106251-2106260.
[34] A. Chroni, T. Mavromoustakos, S. Pispas Poly(2-oxazoline)-Based Amphiphilic Gradient Copolymers as Nanocarriers for Losartan: Insights into Drug–Polymer Interactions *Macromol* **2021**, *1*, 177-200.
[35] Y. Milonaki, E. Kaditi, S. Pispas, C. Demetzos Amphiphilic gradient copolymers of 2-methyl- and 2-phenyl-2-oxazoline: self-organization in aqueous media and drug encapsulation *J Polym Sci, Part A: Polym Chem* **2012**, *50*, 1226-1237.
[36] S. Thayumanasundaram, T. R. Venkatesan, A. Ousset, K. Van Hollebeke, L. Aerts, M. Wubbenhorst, G. Van den Mooter Complementarity of mDSC, DMA, and DRS Techniques in the Study of T_g and Sub-T_g Transitions in Amorphous Solids: PVPVA, Indomethacin, and Amorphous Solid Dispersions Based on Indomethacin/PVPVA *Mol Pharm* **2022**, *19*, 2299-2315.
[37] J. Zhang, R. Thakkar, Y. Zhang, M. Maniruzzaman Microwave induced dielectric heating for the on-demand development of indomethacin amorphous solid dispersion tablets *J Drug Deliv Sci Technol* **2021**, *61*, 102109-102119.
[38] P. Srinivasan, M. Almutairi, A. A. A. Youssef, A. Almotairy, S. Bandari, M. A. Repka Numerical simulation of five different screw configurations used during the preparation of hot-melt extruded Kollidon® and Soluplus® based amorphous solid dispersions containing indomethacin *J Drug Deliv Sci Technol* **2023**, *85*, 104561-104569.
[39] H. Witte, W. Seeliger Simple synthesis of 2-substituted 2-oxazolines and 5, 6-dihydro-4H-1, 3-oxazines *Angew Chem, Int Ed Engl* **1972**, *11*, 287-288.
[40] N. Solanki, S. S. Gupta, A. T. M. Serajuddin Rheological analysis of itraconazole-polymer mixtures to determine optimal melt extrusion temperature for development of amorphous solid dispersion *Eur J Pharm Sci* **2018**, *111*, 482-491.
[41] T. Gottschalk, B. Gronniger, E. Ludwig, F. Wolbert, T. Feuerbach, G. Sadowski, M. Thommes Influence of process temperature and residence time on the manufacturing of amorphous solid dispersions in hot melt extrusion *Pharm Dev Technol* **2022**, *27*, 313-318.
[42] K. Masuda, S. Tabata, H. Kono, Y. Sakata, T. Hayase, E. Yonemochi, K. Terada Solid-state 13C NMR study of indomethacin polymorphism *Int J Pharm* **2006**, *318*, 146-153.
[43] A. Rusdin, A. Mohd Gazzali, N. Ain Thomas, S. Megantara, D. L. Aulifa, A. Budiman, M. Muchtaridi Advancing Drug Delivery Paradigms: Polyvinyl Pyrolidone (PVP)-Based Amorphous Solid Dispersion for Enhanced Physicochemical Properties and Therapeutic Efficacy *Polymers* **2024**, *16*, 286-311.

[44] M. M. Knopp, N. E. Olesen, P. Holm, P. Langguth, R. Holm, T. Rades Influence of Polymer Molecular Weight on Drug-Polymer Solubility: A Comparison between Experimentally Determined Solubility in PVP and Prediction Derived from Solubility in Monomer *J Pharm Sci* **2015**, *104*, 2905-2912.
[45] J. Wu, G. Van den Mooter The influence of hydrogen bonding between different crystallization tendency drugs and PVPVA on the stability of amorphous solid dispersions *Int J Pharm* **2023**, *646*, 123440-123447.
[46] I. C. B. Martins, A. S. Larsen, A. O. Madsen, O. A. Frederiksen, A. Correia, K. M. O. Jensen, H. S. Jeppesen, T. Rades Unveiling polyamorphism and polyamorphic interconversions in pharmaceuticals: the peculiar case of hydrochlorothiazide *Chem Sci* **2023**, *14*, 11447-11455.
[47] C. A. Angell, P. H. Poole, J. Shao Glass-forming liquids, anomalous liquids, and polyamorphism in liquids and biopolymers *Il Nuovo Cimento D* **1994**, *16*, 993-1025.
[48] A. Newman, G. Zografi Considerations in the Development of Physically Stable High Drug Load API- Polymer Amorphous Solid Dispersions in the Glassy State *J Pharm Sci* **2023**, *112*, 8-18.
[49] X. Yuan, T. X. Xiang, B. D. Anderson, E. J. Munson Hydrogen Bonding Interactions in Amorphous Indomethacin and Its Amorphous Solid Dispersions with Poly(vinylpyrrolidone) and Poly(vinylpyrrolidone-co-vinyl acetate) Studied Using (13)C Solid-State NMR *Mol Pharm* **2015**, *12*, 4518-4528.
[50] T. J. Kistenmacher, R. E. Marsh Crystal and molecular structure of an antiinflammatory agent, indomethacin, 1-(p-chlorobenzoyl)-5-methoxy-2-methylindole-3-acetic acid. *J Am Chem Soc* **1972**, *94*, 1340−1345.
[51] C. J. Strachan, T. Rades, K. C. Gordon A theoretical and spectroscopic study of gamma-crystalline and amorphous indometacin *J Pharm Pharmacol* **2007**, *59*, 261-269.
[52] T. Matsumoto, G. Zografi Physical properties of solid molecular dispersions of indomethacin with poly(vinylpyrrolidone) and poly(vinylpyrrolidone-co-vinyl-acetate) in relation to indomethacin crystallization *Pharm Res* **1999**, *16*, 1722-1728.
[53] G. Van den Mooter The use of amorphous solid dispersions: A formulation strategy to overcome poor solubility and dissolution rate *Drug Discov Today Technol* **2012**, *9*, e71-e85.
[54] Y. Li, J. Rantanen, M. Yang, A. Bohr Molecular structure and impact of amorphization strategies on intrinsic dissolution of spray dried indomethacin *Eur J Pharm Sci* **2019**, *129*, 1-9.
[55] S. Saboo, D. E. Moseson, U. S. Kestur, L. S. Taylor Patterns of drug release as a function of drug loading from amorphous solid dispersions: A comparison of five different polymers *Eur J Pharm Sci* **2020**, *155*, 105514-105528.
[56] A.-L. Ziegler, Master thesis, University of Würzburg **2022**.
[57] E. Komarczuk, Master thesis, University of Helsinki **2022**.
[58] D. Hwang, T. Dismuke, A. Tikunov, E. P. Rosen, J. R. Kagel, J. D. Ramsey, C. Lim, W. Zamboni, A. V. Kabanov, T. R. Gershon, D. M. Sokolsky-Papkov Ph Poly(2-oxazoline) nanoparticle delivery enhances the therapeutic potential of vismodegib for medulloblastoma by improving CNS pharmacokinetics and reducing systemic toxicity *Nanomed* **2021**, *32*, 102345-102356.